Magnetic Resonance Imaging 56 (2019) 77–85

Contents lists available at ScienceDirect

Magnetic Resonance Imaging

journal homepage: www.elsevier.com/locate/mri

Original contribution

Application of low-field, $^{1}H/^{13}C$ high-field solution and solid state NMR for characterisation of oil fractions responsible for wettability change in sandstones

Igor Shikhov[a,*], Donald S. Thomas[b], Aditya Rawal[b], Yin Yao[c], Bulat Gizatullin[d], James M. Hook[b], Siegfried Stapf[d], Christoph H. Arns[a]

[a] School of Mineral and Energy Resources Engineering, The University of New South Wales, Sydney, 2052 NSW, Australia
[b] Nuclear Magnetic Resonance Facility, UNSW Mark Wainwright Analytical Centre, Sydney, 2052 NSW, Australia
[c] Electron Microscopy Unit, UNSW Mark Wainwright Analytical Centre, Sydney, 2052 NSW, Australia
[d] FG Technische Physik II/Polymerphysik, Technische Universität Ilmenau, D-98684 Ilmenau, Germany

ARTICLE INFO

Keywords:
Asphaltene adsorption
Ageing
Wettability alteration
NMR relaxometry
Solution-state NMR spectroscopy

MSC:
01-06
Revision v.1

ABSTRACT

Asphaltene adsorption on solid surfaces is a standing problem in petroleum industry. It has an adverse effect on reservoir production and development by changing rock wettability, plugging pore throats, and affects oil transport through pipelines. Asphaltene chemistry constitutes important part of the ageing process as part of petrophysical studies and core analysis. The mechanisms and contribution of various oil components to adsorption processes is not fully understood. To investigate the kinetics of the ageing process and address the relative contribution of different oil components, we prepared three sets of sandstone core plugs aged in different oil mixtures over various time intervals. Cores were then re-saturated with decane to evaluate their wetting state using low-field NMR relaxometry by monitoring a change of surface relaxivity. Adsorbed deposits were then extracted from cores for solution-state NMR analysis. Their ^{1}H and ^{1}H-^{13}C correlation spectra obtained using heteronuclear single quantum coherence (HSQC) technique were matched to spectra of four SARA (saturates, aromatics, resins and asphaltenes) components of oil mixtures to deduce components of deposits and inter-component interactions. We notice that wettability reversal of rock is inversely proportional to initial asphaltene concentration. Analysis of deposits reveals an increase in their aliphatic content over ageing time, which is accompanied by a change of the morphology of the pore space due to cluster aggregates forming a network. Results suggest that the ageing process in respect to the wetting state of rock samples consists of three distinctive stages: (i) an early-time period, when the fraction of most polar asphaltenes creates a discontinuous layer corresponding to mixed-wet state; (ii) an intermediate-time interval, at which the full grain coverage may be achieved (at favourable chemical environment) corresponding to strong oil-wetting; (iii) a late-time stage, where intense macro-aggregates accumulation occurs, changing the pore space integrity. It is likely asphaltene-aliphatic interactions leading to growth of sub-micron size macro-aggregates.

1. Introduction

Asphaltenes are the most active and least understood class of natural hydrocarbons, causing major issues in hydrocarbon production and transportation. At certain conditions, asphaltenes may precipitate on solid surfaces, changing their wetting properties [1], and being accumulated, create restrictions to flow [2]. On the positive side, controlled asphaltene precipitation on mixed-layer clays may be utilised to prevent clay swelling, contributing to production enhancement. Petroleum reservoir characterisation involve laboratory core analysis, which requires restoration of the original core wettability state. This is achieved by setting a core to a water-wet state, followed by a wettability alteration step by exposing a rock sample to crude oil at elevated temperature (ageing process). The inherent problem of the ageing step is due to the need to mimic a natural process which takes tens of million years in a time-scale of a few months, and partly due to the limited understanding of both fluid-solid and fluid-fluid interactions between oil components. Developments in NMR technology enable monitoring the dynamics of the wettability state of cores [3,4]. High-field NMR spectroscopy offers well-established analytical techniques to study the

* Corresponding author.
E-mail address: igor.shikhov@unsw.edu.au (I. Shikhov).

https://doi.org/10.1016/j.mri.2018.10.004
Received 31 August 2018; Received in revised form 5 October 2018; Accepted 6 October 2018

Table 1
Ageing schedule of Bentheimer core samples.

Step/rock sample no.[a]	1	2	3	4	5	6	7	8	9	10	11	12
Total ageing time, t_a [days]	4	5.5	7.5	10	13	17	22	28	36	52	72	100

[a] Each time step corresponds to a different core, total of 12 in each set aged in oil OM.1, -2 or -3.

chemical structure of hydrocarbons and interactions between their components [5,6]. We combine low-field NMR relaxation techniques and high-field chemical shift spectroscopy to investigate the role of interactions between asphaltene and SAR components of oil during the ageing process of rock cores by monitoring the evolution of wettability and the composition of adsorbed deposits.

1.1. Reactivity of asphaltenes and wettability

Crude oils can be defined as a solution of polar components (resins and asphaltenes) in a non-polar solvent (saturates and aromatics). Asphaltenes are defined as an insoluble fraction of oil in alkanes and soluble in basic aromatic solvents [7]. Asphaltene molecules are represented by polyaromatic hydrocarbon (PAH) cores enriched with heteroatom groups, several of which are polar (− SH, − OH, − NH) or charged (e.g. carboxyl, − COOH). Trace amount of metals (V, Fe, Ni) play an important role in asphaltene association. Wettability is one of the main factors governing oil recovery since it controls initial fluids distribution, capillary pressure and relative permeability. The role of asphaltenes in wettability reversal is long known [8]. It has been reported that asphaltenes reactivity (tendency to flocculate and adsorb on solid surfaces) correlates to various features in their structure (e.g. metal content and polarity) and solvent properties. The size of PAH cores in asphaltene molecules is also a factor increasing the tendency of aggregation [9].

1.2. Scope

In this work we investigate the relationship between oil composition, interactions between asphaltene and other oil components, adsorption rate and wettability change of the rock by an ageing process. Three sets of Bentheimer sandstone core plugs were aged in different oil mixtures over various time intervals, cleaned and subsequently re-saturated with decane. We use low field NMR T_2 relaxation measurements to monitor the wettability evolution via surface relaxivity dynamics. ^{1}H solution-state and single-bond correlation (HSQC) spectra of deposits eluted from aged plugs were compared to those of four SARA components of ageing oils to deduce the composition of deposits. ^{13}C solution-state and solid-state DP MAS ^{13}C spectra were used to evaluate asphaltene structure. NMR low-field relaxometry and a set of spectroscopic techniques enable observing relationship between rock wettability and the chemistry of the adsorption process; in particular we detect a significant asphaltene-maltene interactions at the later stage of ageing.

2. Materials: rock samples and oils

2.1. Rock cores

We prepared three sets of 12 rock core plugs (32–34 mm long and 12.7 mm diameter) for ageing and spare two more plugs for reference. The cores originate from an outcrop Lower Cretacious formation in Bad Bentheim, Germany. Bentheimer is a clean sandstone (quartz arenite) composed mainly of quarts grains (95.9 vol %), kaolinite (1.6 vol %) and feldspar (2.5 vol %). The mean porosity of Bentheimer plugs is 23.9%, permeability to brine measured on larger cores is 1.3 Darcy. This sandstone is weakly diamagnetic.

Specific surface area of Bentheimer sandstone determined using BET gas adsorption method is 0.45 m^2/g [11]. A small volumetric fraction of kaolinite contributes more than 50% of that value – 0.25 m^2/g (assuming a value of 17 m^2/g for kaolinite phase). BET surface area can be regarded as an upper bound value. On the other end are values obtained using MICP, e.g. Mitchell and Fordham [12] – 0.043 m^2/g and by micro-CT image analysis, Shikhov et al. [13] – 0.056 m^2/g.

2.2. Petroleum fluids

We prepared three oil mixtures (or synthetic oils) for the ageing process. The main source of asphaltenes in the oil mixtures is commercial grade C170 bitumen. Asphaltene's weight fraction in bitumen is about 17%, depending on the method used (Table 2), in crude oil 1.5–3.5% and in oil mixtures 1.6–3.9 wt%. The remaining parts of the mixtures are n-hexadecane (99.97% purity) and toluene (99.8%). The physical properties and composition of the oil mixtures are summarised in Table 3 and Table 4 respectively.

2.3. Ageing protocol

Initially, three sets of dry rock samples were fully saturated with one of the oil mixtures OM.1–3 using a desiccator connected to a vacuum line. Saturated samples were placed in 20 cc vials containing 10 mL of oil, sealed and placed into the oven at 60 °C for a period of ageing time following the time schedule, Table 1. Thus, each sample was aged once for a scheduled ageing time interval, while the whole set naturally captures the dynamics of ageing and adsorption. After ageing the cores were cleaned by soaking in n-hexane for six days, while solvent was replaced with fresh n-hexane every 12 h. This procedure was performed at ambient lab temperature of 22 °C.

Fig. 1 shows the arrangement of cores into three sets aged in different oils. Pictures were taken after cores were cleaned and dried. Note, the cores in the upper row (aged in the oil with low asphaltene content) are darker, than those aged in oils containing higher asphaltene fractions. This counterintuitive observation is in line with field experience - reservoirs with oils having asphaltene concentration above a certain value have no deposition issues, while small asphaltene concentration may be problematic. A systematic study of Haji-Akbari et al. [14] on relationship between asphaltene concentration and their aggregation tendency found that higher concentration (above 1 wt%) have a stabilising effect on aggregation, thus decreasing amount of species available to precipitation.

Table 2
SARA analysis of bitumen.

Hydrocarbons	Saturates, wt%	Aromatics, wt%	Resins, wt%	Asphaltenes, wt%	Volatiles + LOC[c], wt%
Bitumen, IP469[a]	12.90	28.80	41.68	15.72	0.90
Bitumen, D2007[b]	26.59	34.03	15.44	17.87	6.07

[a] Energy Institute IP469 standard describes TLC-FID technique/Iatroscan technology.
[b] ASTM D2007 standard describes sequential flushing chromatography.
[c] LOC - loss on column. Applies to the IP469 method due to oil topping at 250 °C prior to TLC-FID and to D2007 method because of solvent removal at 60 °C.

Table 3
Physical properties of oils.

Hydrocarbons	Density, g/cc @ 22 °C	Density, g/cc @ 35 °C	Viscosity, cP @ 22 °C	Viscosity, cP @ 35 °C	TAN[a], mg KOH/g	TBN[a], mg KOH/g
OM.3	0.8792	0.8554	3.61	3.09	2.37	1.00
OM.2	0.8529	0.8470	2.42	2.03	1.14	0.78
OM.1	0.8240	0.8162	1.78	1.54	1.63	0.32

[a] TAN - Total Acid Number and TBN - Total Base Number expressed in equivalent of KOH concentration.

Table 4
Components of oil mixtures.

Oil and mixtures	Bitumen, wt%	Crude oil, wt %	$C_{16}H_{34}$, wt%	Toluene, wt%
OM.1	10.0	0.0	50.0	40.0
OM.2	15.0	30.0	15.0	40.0
OM.3	25.0	0.0	40.0	35.0

3. SEM

The Yen-Mullins model of hierarchical asphaltene aggregation is now widely accepted [15-17]. The model postulates that single-PAH "island" asphaltene molecules depending on concentration may form small aggregates of < 10 molecules, which in turn may form small clusters of < 10 aggregates. It is stressed that the size of these structures may not exceed approximately 5 nm unless the planar surface of clusters is modified by other compounds. There are numerous experimental confirmations of the model in literature, e.g. Zhang et al. [18]. There is no detailed theory proposed to explain the formation of larger aggregates (medium-size of about 50 nm, large fractal of about 100 to 300 nm and even larger of about 1 μm) reported in literature, e.g. Tanaka et al. [19], Behbahani et al. [16].

We obtained several SEM images of cores aged for 52 days. Close examination of images reveals three characteristic sizes/types of the nearly spherical particles in deposits, see Table 5. Fig. 2 [a, d] shows large scale highly porous aggregate structures. Some accumulations exhibit two types of particles, e.g. Fig. 2 [b, c] shows 'medium' size 500 nm particles connected with narrow bridges and 'large' particles of 1.5 μm with thick bridges. Higher magnification images clearly show that these particles are made of smaller ones of about 20 to 50 nm, Fig. 2 [e, f].

4. NMR techniques to asphaltene characterisation

4.1. Low-field NMR relaxometry

Transverse relaxation responses of decane saturating variously aged Bentheimer core plugs were obtained using a 2 MHz Magritek Rock Core Analyzer utilising a standard Carr-Purcell-Meiboom-Gill (CPMG) technique [20,21]. The CPMG pulse sequence consists of an initial excitation 90° pulse, followed by a series of re-focusing 180° pulses having inter-pulse time interval (echo time t_E) of 200 μs. The number of echoes (40,000) was selected to be sufficient to resolve the longest relaxation component. The top of each echo was acquired providing a magnetisation decay governed by transverse relaxation processes. The inversion problem of obtaining eigenvalues for an observable integral signal with assumed multi-exponential kernel has been solved by a 1D inverse Laplace transform (ILT) with non-negativity constraint and L-curve smoothing criterion following Lawson and Hansen [22]. The repetition time between scans was 60 s to ensure thermal equilibration of a system (primarily due to hardware requirements).

Fig. 3 [a–c] shows three time series of T_2 distributions obtained on aged core plugs saturated with decane. Note the strong shift of distributions towards shorter relaxation times with ageing time increase for the set aged in oil mixture OM.2, while the shift is more moderate for the set aged in OM.1, and very limited in case of OM.3 (visible only last two distributions). Relaxivity was calculated by matching the log-mean MICP pore-aperture and T_2 relaxation time distribution assuming the motional-averaging regime and negligible internal gradient effects.

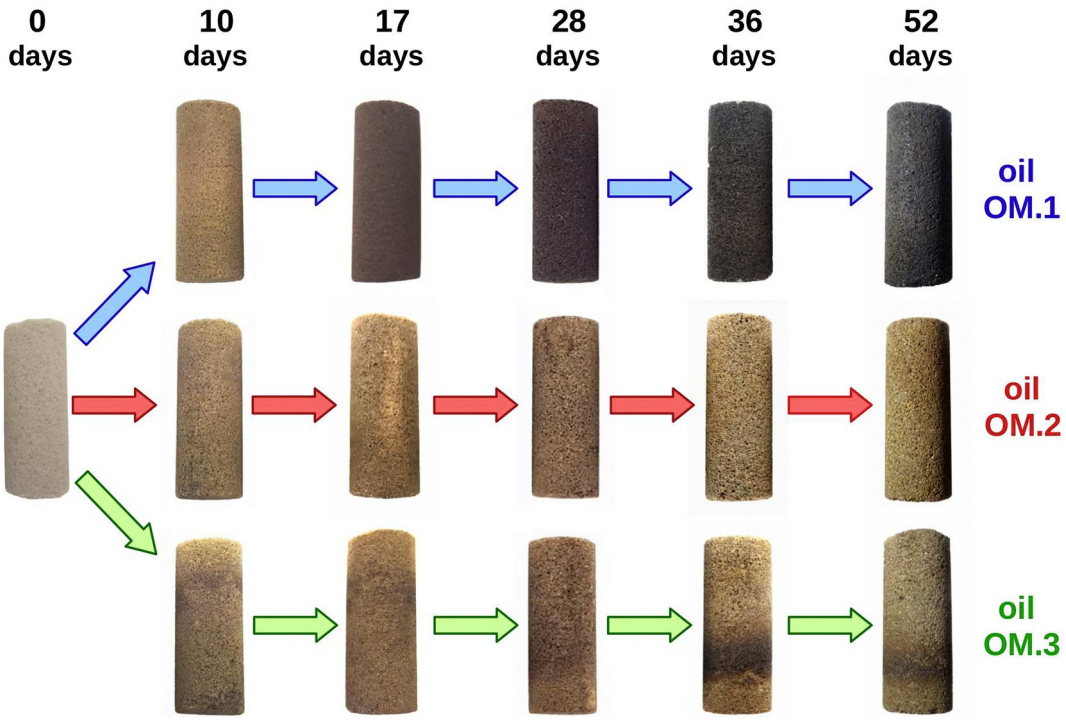

Fig. 1. Arrangement of Bentheimer cores into three sets aged in different oils (actually, 12 cores per set, Table 1).

Table 5
Types of globules in deposited macro-aggregates.

Deposit type	Particle size, nm	Bridge type	Porosity
I. (fine)	200–300	Thin	High
II. (medium)	500–600	Thin	High
III. (coarse)	850–1250	Thick	Medium

Observed surface relaxivity is translated to NMR wettability index following conceptually works of Fleury and Deflandre [4], Looyestijn and Hofman [23], and Chen et al. [24], as follows:

$$I_{NMR}(t_a) = I_w - I_o = \frac{2(\rho_{ow} - \rho_2(t_a))}{\rho_{ow} - \rho_{ww}} - 1, \quad (1)$$

where $\rho_2(t_a)$ is the observed surface relaxivity estimated for decane-

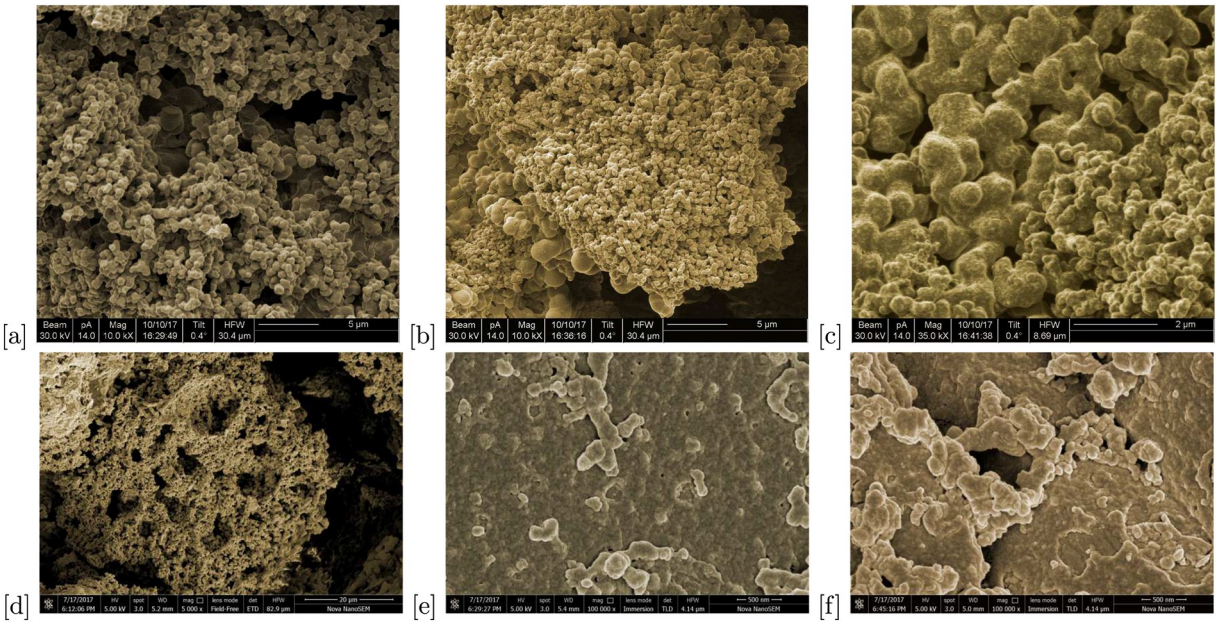

Fig. 2. SEM images capturing various types of aggregates in the cores aged for 52 days: [a, d] accumulations of high and multi-scale porosity; [b, c] evidence of two particle types; [e, f] high-magnification images of globules made of 20–50 nm clusters.

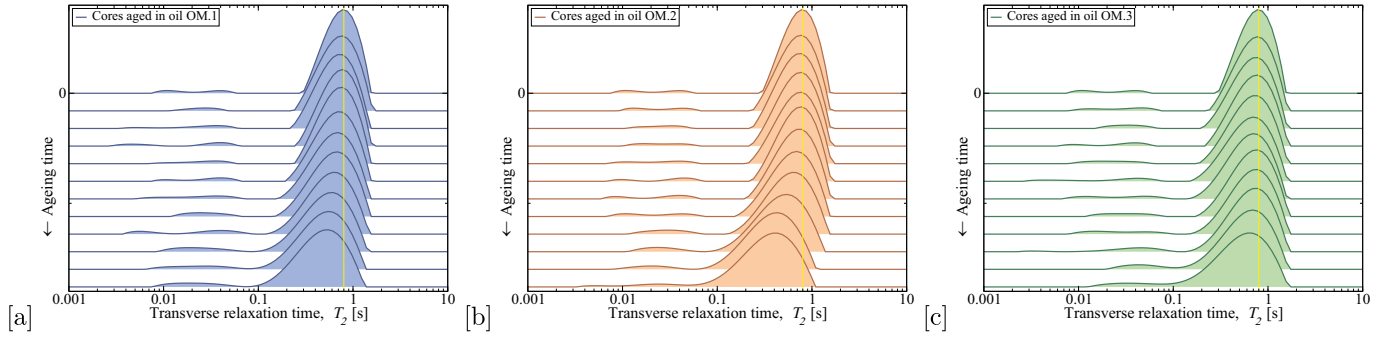

Fig. 3. Relaxation time distributions of decane saturated Bentheimer cores aged in oils OM.1–3 over specified time intervals following Table 1. The reference line at 800 ms corresponds to the mode of T_2 distribution of a core before ageing.

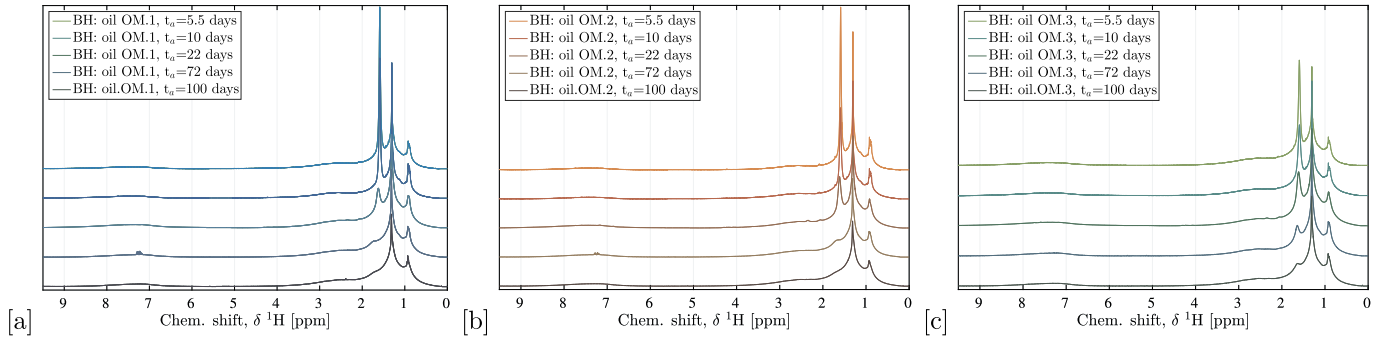

Fig. 4. Proton NMR spectra of deposits eluted from Bentheimer cores aged in three oil mixtures over five time intervals. DCM calibration peaks at 5.32 ppm are removed.

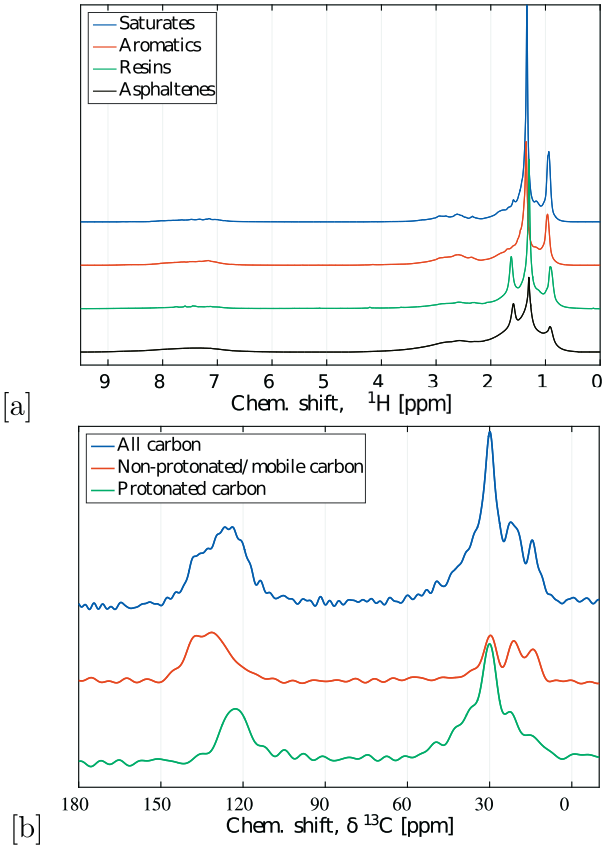

Fig. 5. [a] Solution-state ^{1}H spectra of SARA components extracted from bitumen. DCM peaks at 5.32 ppm are removed. [b] Quantitative ^{13}C solid state 12 kHz DP MAS NMR spectra of asphaltenes extracted from bitumen.

saturated core after it underwent ageing over time t_a, where ρ_{ww} is the surface relaxivity of a strongly water-wet core ($I_{NMR} = 1$) and ρ_{ow} is the surface relaxivity of a strongly oil-wet core ($I_{NMR} = -1$).

The main assumption in this model is a linear relationship between relaxivity and wettability change. Comparing to other published models this one is more simplistic and implicit since we use only oil phase in our experiments (n-decane), thus, evaluating water wetness indirectly. The enhancement of relaxation due to bulk accumulations and approach to estimate their contribution was demonstrated in our recent work [25]. To exclude the influence of bulk accumulations on wettability estimated from NMR relaxation, here we truncated data beyond 28 days of ageing, assuming $\rho_{ow} = 7.0$ μm/s.

4.2. Solution-state ^{1}H NMR spectroscopy

Proton NMR is regularly used to characterise crude oils and analyse their SARA fractions [26,27]. High-resolution solution-state proton NMR spectra of oils SARA components and deposits were obtained using a Bruker Avance III spectrometer operating at a static magnetic field of 9.4 T(400.13 MHz ^{1}H resonant frequency). Samples were prepared by dissolving 6 to 8 mg of a dry precipitant in 0.6 mL of dichloromethane-d_2. Chemical shift ^{1}H spectra of SARA components and deposits eluted from cores were recorded at 25 °C temperature via lock channel with 65,536 data points, a sweep width 12 ppm (4800 Hz) and a relaxation delay (inter-scan time) of 5.0 s. 32 scans were acquired giving a total acquisition time of about 6 1/2 min.

The contribution of different species to ^{1}H NMR spectra of SARA fractions, Fig. 5[a], was evaluated following published chemical shift assignments [28,29]. Spectra contain two groups of peaks corresponding to (a) protons in mono- and multi-aromatic rings in the 6.0–9.5 ppm range of chemical shifts and (b) aliphatic protons of 0.5–4.5 ppm. The right-most peak at 0.9 ppm corresponds to terminal alkyl groups at the end of paraffin chains attached to PAH. Protons of methyl groups next to aromatic rings exhibit a chemical shift mainly in the 2–3 ppm interval, with the tail extending up to 4.5 ppm. The largest peak at about 1.3 ppm - are protons in CH_2 of alkane chains attached to aromatic groups. Naphthenic protons in the vicinity of aromatic rings (typically in γ position) and tertiary alkyl CH in β position contribute to 1.6 ppm shift. One prominent difference between spectra of SARA components is a difference of 0.9, 1.3 and 1.6 ppm peak contributions: from saturates to aromatics and further to resins and asphaltenes the fraction of 0.9 (terminal CH_3) decreases, while the contribution of 1.6 ppm peak increases. This peak is also clearly larger in asphaltenes compared to resins. We use this feature in the analysis of deposits composition.

4.3. Solid-state ^{13}C DP/MAS NMR

High-resolution solid-state ^{13}C NMR spectrum of asphaltene was acquired with direct-polarization magic-angle spinning (DP/MAS) NMR using a Bruker Avance III spectrometer operating at a static magnetic field of 7 T(75 MHz and 300 MHz resonant frequency for ^{13}C and ^{1}H respectively). The sample was packed into a 4-mm (o.d.) zirconia rotor and spun at 12 kHz. ^{13}C-90° pulse length of 4.5 μs with a Hahn echo prior to detection were used along with 80 kHz of ^{1}H SPINAL-64 decoupling [30]. Recycle delays of 30 s were allowed to ensure full signal relaxation and 832 transients were co-added to achieve sufficient signal to noise. Application of DP/MAS NMR allows to quantify aromaticity of complex hydrocarbon molecules and non-protonated carbons [31], detection of alkyl functional groups and provides a valuable tool in the reconstruction of complex molecular structures. We consulted several recent works to create ^{13}C assignments to quantify structural parameters, e.g. Siskin et al. [32], Silva et al. [28]. Fig. 3[b] shows quantitative spectra used to deduce fractions of carbons in specific environments.

Both ^{1}H and ^{13}C spectra can be used to determine the ratios of hydrogen and carbon atoms each contributing to aliphatic and aromatic parts of asphaltene molecules. The results of such calculations can be used to estimate the number of aromatic rings and the number of peripheral aliphatic chains from which an approximate chemical formula can be predicted for each sample. We can estimate that a typical asphaltene molecule contains some 8 cyclic carbon rings mostly aromatic with few alyphatic chains (propyl on average) and may include a carbonyl group. The molecular weight of such a molecule is 600 to 700 Da. However, in the absence of reliable mass spectrometry data our conclusions are approximate.

4.4. HSQC NMR

Two-dimensional (2D) NMR correlation spectroscopic techniques enable more reliable and specific assignments. The HSQC (Hetero-nuclear Single Quantum Coherence) pulse sequence is an inverse detected (observed via the ^{1}H nucleus) two-dimensional heteronuclear correlation experiment, where the resulting spectrum has ^{1}H chemical shifts in one dimension and chemical shifts of magnetically active ^{13}C heteronuclei connected to hydrogen by a single bond in the second dimension. The adiabatic edited ^{1}H-^{13}C HSQC experiments [33] were acquired with 2048 data points in the ^{1}H domain and 128 transients in the indirect dimension of ^{13}C, Fig. 6. We use a sweep width of 12 ppm in the ^{1}H dimension and 190 ppm in the ^{13}C dimension. ^{1}H acquisition time was 212 ms and ^{13}C acquisition time 3 ms. The ^{1}H excitation pulse was calibrated to 12 μs and a $^1J_{HC}$ coupling constant of 145 Hz was used. Chemical shift was calibrated to the residual dichloromethane peak (^{1}H 5.32 ppm, ^{13}C 53.84 ppm). The presence of several overlapping peaks were confirmed by HSQC.

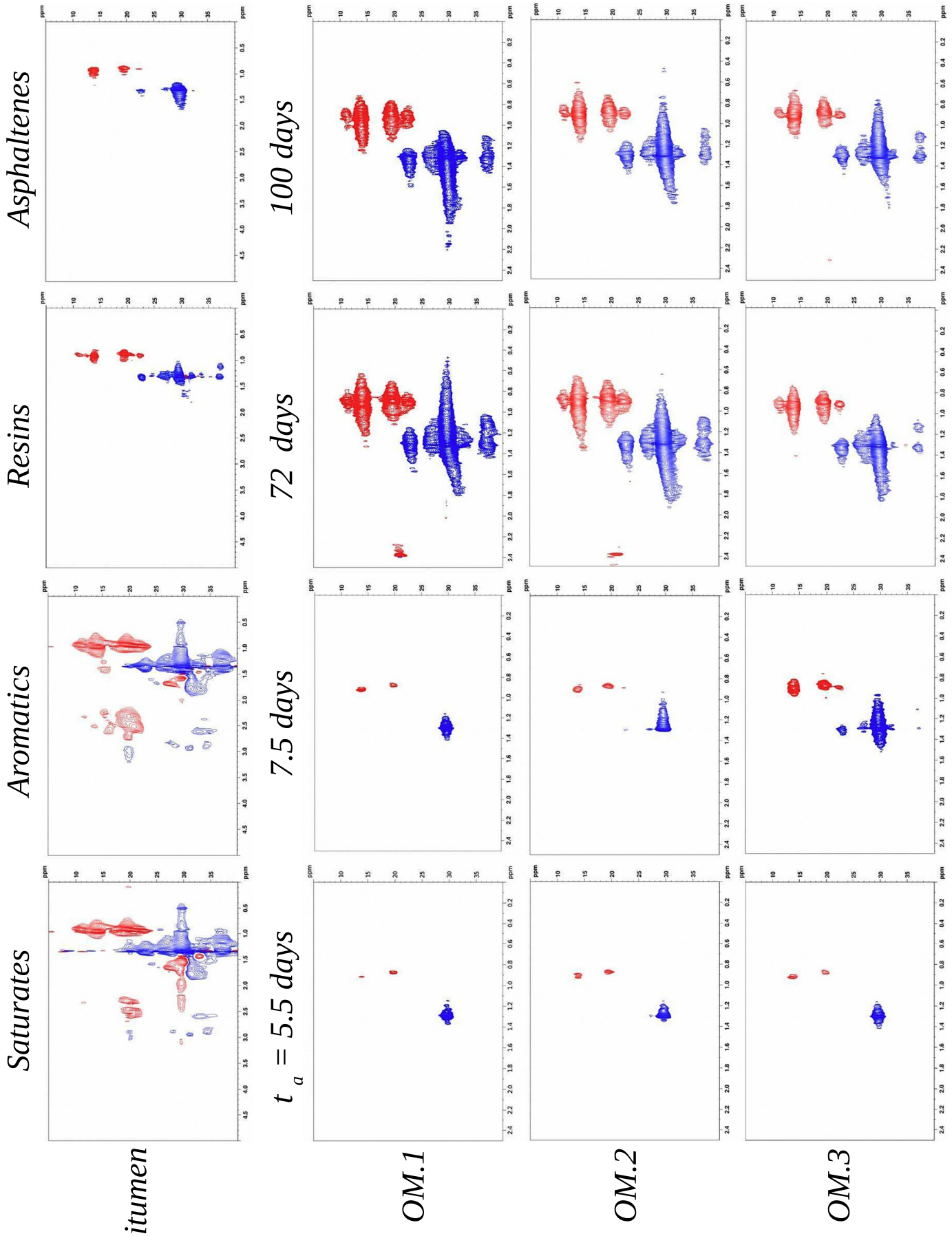

Fig. 6. Aliphatic region of liquid-state ^{1}H-$^{13}HSQC$ NMR spectra: the upper row - SARA components of bitumen; the lower three rows - deposits eluted from Bentheimer aged cores.

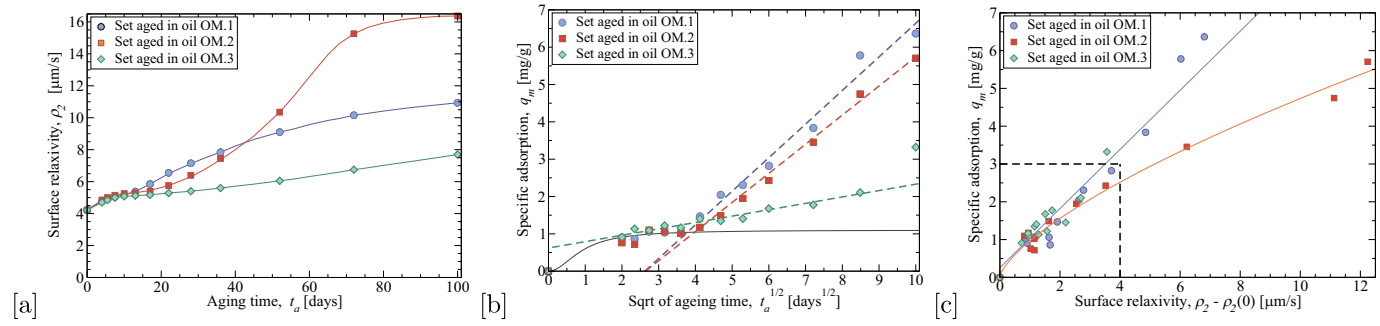

Fig. 7. [a] Evolution of surface relaxivity of variously aged cores. [b] Specific adsorption q_m fitted with two nested kinetic models - PSO (solid black line) and IPD (dash lines). [c] Surface relaxivity change plotted versus specific adsorption q_m. A region limited by black dash lines shows a near linear common trend.

5. Results

Fig. 7[a] shows the evolution of surface relaxivity for three sets of cores aged up to 100 days. The rate of relaxivity change varies strongly between the three sets and in case of a set aged in oil OM.2 is strongly non-linear. The degree of relaxation enhancement over the whole ageing time interval is factor ×4.0 (OM.1), ×2.7 (OM.2) and ×1.9 (OM.3). The same data fitted with bi-component kinetic model (pseudo-second order, PSO [34] and intraparticle diffusion, IPD [35]) is shown on Fig. 7[b]. Interestingly, the three sets exhibit a similar equilibrium adsorption value of 1 mg/g according to the PSO model and distinctively different adsorption rates following IPD. Indeed, IDP adsorption constants k_d correlate with bulk diffusion coefficients of oils, Table 6. Fig. 7[c] demonstrates a plot of surface relaxivity versus specific adsorption q_m. A near linear common trend limited by the black dash line corresponds to equilibrium time according to the PSO model.

It is important to stress that the results may change significantly if different experimental conditions and rock were used. In particular, a change in temperature would speed up or slow down the reactions and diffusion coefficients of oil components, changing duration and rates of ageing stages. Mineralogy, specific surface area and surface roughness are among the main governing factors defining rate of deposit accumulation. Specific surface area affects more the second, diffusion limited process and the surface roughness is more important factor in the first, reaction limited stage.

Fig. 8[c] shows the evolution of relaxation-based wettability index calculated on reduced to 28 days time interval. The three characteristic time-intervals include an early-time relatively quick change to mixed or intermediate wetting state, followed by a period of stable wetting state of the same length of 5–7 days and ultimately by change towards the strong oil-wetness (for oils OM.1 and OM.2 only). Comparing the specific adsorption q_m and surface relaxivity ρ_2 time-series of aged cores, Fig. 7 [a, b], to corresponding proton chemical shift spectra of deposits, Fig. 4, one can see the inverse correlation between both q_m and ρ_2 to amplitude of the initially significant peak of δ at about 1.6 ppm. The trend is consistent for all three sets aged with the different oil mixtures. The plot of 1.6 ppm shift fraction in deposits proton spectra versus surface relaxivity ρ_2 of corresponding core is shown on Fig. 8[a]. Two asymptotic near linear regimes of surface relaxivity ρ_2 to $\delta_{1.6\ ppm}$ relationship are evident from the plot: one corresponds to early time ageing, when the fast decrease of $\delta_{1.6\ ppm}$ over the limited range of ρ_2 occurs, followed by the inflection point after which the growth of surface relaxivity shows no dependence on $\delta_{1.6\ ppm}$, which remains practically constant. By assuming that the ^{1}H spectra of deposits could be represented by a sum of two components - asphaltene and one of SAR fractions or solvent component in the oil mixture such as hexadecane or toluene, we performed fitting by minimising amplitude residue of five spectra components of deposit spectra (aromatic, α-, β- and γ-aliphatic, and β-naphthenic protons).

The best matching pairs are asphaltene/saturate and asphaltene/resin components of bitumen. A weight fraction of non-asphaltenic content of deposits is presented as an area limited by a maximum fraction of resin content and a minimum fraction of aliphatic content, Fig. 8[b]. The fitting function is in the form of $\log t_a + b$. Note, that initially deposits are made of pure asphaltenes followed by a period of fast increase of non-asphaltene content (until t_a = 22 days) after which the growth become more steady. The same approach was applied to HSQC spectra (by comparing integrated amplitude of nine peaks), which confirms the presence of either saturates or resins in late-time deposits, Fig. 9.

Table 6
IDP rate constants vs self-diffusion coefficients.

Oil mixtures	OM.1	OM.2	OM.3
D_0, 10^3 μm^2/s	0.61	0.51	0.38
k_d, mg/g/day$^{1/2}$	0.90	0.78	0.17

6. Discussion and conclusion

By combining results provided by low-field relaxometry and high-field spectroscopy we observed the existence of three phenomenologically different stages of the ageing process, where interaction of oil components with rock solids subjected to subsequent flushing by light alkane leads to distinctive wetting and morphological conditions:

(i) the fast increase of oil wetness towards intermediate wetting state by formation of a partially continuous layer of high-polar asphaltenes with none to low non-asphaltene content); Among the main reasons of a layer discontinuity is solid topology (surface roughness): occurs over first 5 to 7 days;
(ii) the longer intermediate period, which depending on oil composition may lead to a shift towards the strong oil-wetness; At this stage the withdrawal from the solution of the most polar asphaltenic compounds is continuing. The less polar oil exposed to hexane at lower temperature during the rinsing step starts forming the aliphatic-rich thicker layer made of asphaltene/aliphatic micelles. It occurs between 5 and 20 days of ageing.
(iii) the late stage - further layer growth accompanied with trapping of large porous macro-aggregates hundreds nm across (partly during flashing step at certain morphological conditions within the core). The deposited aggregates remain ordered so that molecules containing metal porphyrins provide increasingly efficient relaxation environment (more effective than rock solid surface). Together with morphological change this lead to increase of apparent surface relaxivity, however, without actual increase of surface oil wetness.

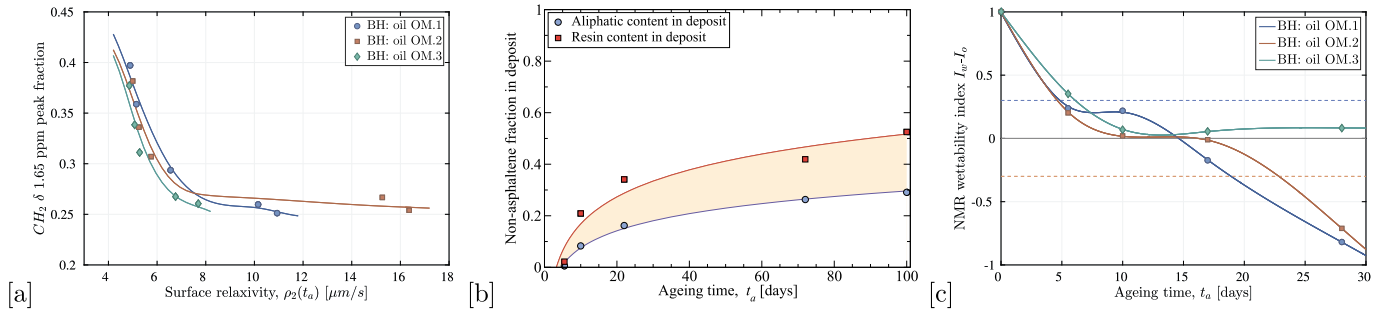

Fig. 8. [a] Plot of surface relaxivity versus 1.6 ppm peak intensity of deposit ^{1}H spectra. [b] Non-asphaltene fraction in deposits eluted from aged cores evaluated using ^{1}H spectra. The upper red curve corresponds to maximum of resin fraction and the lower curve is the minimum of aliphatic fraction. [c] NMR wettability indices calculated for core subsets aged up to 28 days. Interval limited by two dash lines at −0.3 and 0.3 corresponds to neutral or mixed-wet states. (For interpretation of the references to color in this figure legend, the reader is referred to the web version of this article.)

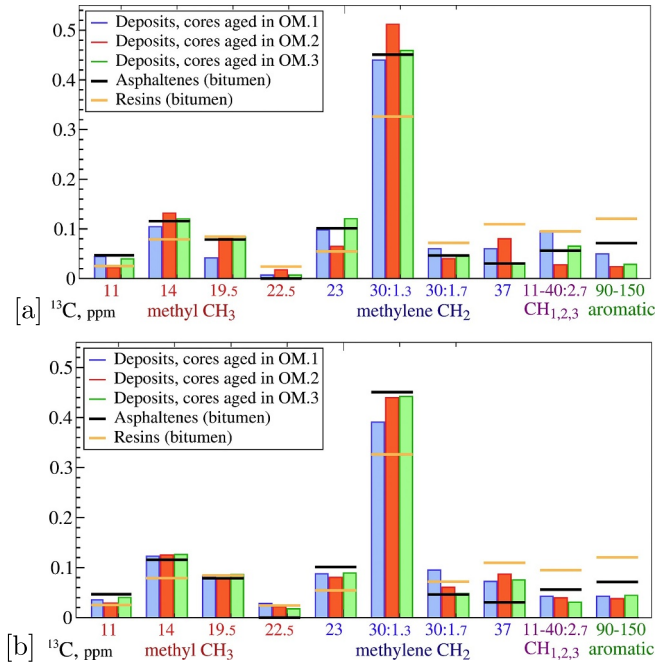

Fig. 9. The bar charts comparing contributions of major peaks to HSQC spectra of [a] deposits eluted from cores aged over 5.5 days and [b] late stage deposits (100 days) to corresponding components of HSQC spectra of resins (the orange horizontal bars) and asphaltenes (black bars). The leftmost four groups of bars correspond to CH and CH_3 and the following four groups are CH_2, both having ^{1}H shift of up to 1.7 ppm. The second group of bars from the right are non-aromatic CH, CH_2 and CH_3 having stronger ^{1}H shift typically of 2.7 and up to 4.5 ppm. (For interpretation of the references to color in this figure legend, the reader is referred to the web version of this article.)

The oil wetness phenomenon in oil-bearing rocks is typically attributed to the interaction between asphaltene functional groups and solid surface polar sites alone. We find that the wettability alteration process considered is governed by factors not limited just to asphaltenes chemistry, but involves their interaction with maltenes, very likely saturates, to form macro-accumulations at a later stage of the ageing process. Such porous aggregates enhance relaxation and consequently can be misinterpreted as an increase of surface relaxivity and accordingly, stronger than actual oil wetness.

The combination of low-field relaxometry and high-field NMR spectroscopy enables to investigate relationship of oil composition and asphaltene chemistry with the wettability of natural rocks, improving the design of laboratory core analysis and petroleum reservoir modelling.

Acknowledgments

The authors acknowledge the Australian Research Council (grant FT120100216) and the member companies of the ANU/UNSW Digital Core Consortium for their support. The authors wish to thank Dr. Rebeya Akter from ICP Laboratory, SSEAU MWAC UNSW for conducting inductively plasma elemental analysis and Dr. Sarah Kelloway from X-ray Fluorescence Laboratory, SSEAU MWAC UNSW for thermogravimetric elemental analysis.

References

[1] Yan J, Plancher H, Morrow N. Wettability changes induced by adsorption of asphaltenes. SPE Prod Facil 1997;12:259–66.
[2] Minssieux L, Nabzar L, Chauveteau G, Longeron D, Bensalem R. Permeability damage due to asphaltene deposition: experimental and modeling aspects. Rev IFP 1998;53:313–27.
[3] Howard J. Quantitative estimates of porous media wettability from proton NMR measurements. Magn Reson Imaging 1998;16:529–33.
[4] Fleury M, Deflandre F. Quantitative evaluation of porous media wettability using NMR relaxometry. Magn Reson Imaging 2003;21:385–7.
[5] Dickinson E. Structural comparison of petroleum fractions using proton and ^{13}C n.m.r. spectroscopy. Fuel 1980;59:290–4.
[6] Majumdar R, Gerken M, Mikula R, Hazendonk P. Validation of the Yen–Mullins model of Athabasca oil-sands asphaltenes using solution-state ^{1}H NMR relaxation and 2D HSQC spectroscopy. Energy Fuels 2013;27:6528–37.
[7] Speight J. The application of spectroscopic techniques to the structural analysis of coal and petroleum. Appl Spectrosc Rev 1971;5:211–63.
[8] Kim S, Boudh-Hir M, Monsoori G. The role of asphaltene in wettability reversal. Proc. SPE Ann. Tech. Conf. & Exhib. New Orleans, USA: SPE 87009; 1990. p. 799–809.
[9] Hortal AE, Hurtado P, Martinez-Haya B, Mullins OC. Molecular-weight distributions of coal and petroleum asphaltenes from laser desorption/ionization experiments. Energy Fuels 2007;21:2863–8.
[11] Peksa A, Wolf K, Zitha P. Bentheimer sandstone revisited for experimental purposes. Mar Pet Geol 2015;67:701–19.
[12] Mitchell J, Fordham E. Contributed review: nuclear magnetic resonance core analysis at 0.3 T. Rev Sci Instrum 2014;85. 111502:1–17.
[13] Shikhov I, d'Eurydice M, Arns J, Arns C. An experimental and numerical study of relative permeability estimates using spatially resolved T_1-z NMR. Transp Porous Media 2017;118:225–50.
[14] Haji-Akbari N, Teeraphapkul P, Fogler H. Effect of asphaltene concentration on the aggregation and precipitation tendency of asphaltenes. Energy Fuels 2014;28:909–19.
[15] Mullins O. The modified Yen model. Energy Fuels 2010;24:2179–207.
[16] Behbahani T, Ghotbi C, Taghikhani V, Shahrabadi A. Investigation of asphaltene adsorption in sandstone core sample during CO_2 injection: experimental and modified modeling. Fuel 2014;133:63–72.
[17] Wang M, Hao Y, Islam M, Chen C. Aggregation thermodynamics for asphaltene precipitation. AIChE J 2016;62:1254–64.
[18] Zhang L, Yang G, Wang J, Li Y, Li L, Yang C. Study on the polarity, solubility, and stacking characteristics of asphaltenes. Fuel 2014;128:366–72.
[19] Tanaka R, Sato E, Araki T. Characterization of asphaltene aggregates using X-ray diffraction and small-angle X-ray scattering. Energy Fuels 2004;18:1118–25.
[20] Carr H, Purcell E. Effects of diffusion on free precession in nuclear magnetic resonance problems. Phys Rev 1954;94:630–8.
[21] Meiboom S, Gill D. Modified spin-echo method for measuring nuclear relaxation times. Rev Sci Instrum 1958;29:688–91.
[22] Lawson CL, Hansen RJ. Solving Least Squares Problems. New-Jersey: Prentice-Hall; 1974.

[23] Looyestijn W, Hofman J. Wettability-index determination by nuclear magnetic resonance. SPE Reserv Eval Eng 2006;9:146–53.
[24] Chen J, Hirasaki G, Flaum M. NMR wettability indices: effect of OBM on wettability and NMR responses. J Petrol Sci Eng 2006;52:161–71.
[25] Shikhov I, Li R, Arns C. Relaxation and relaxation exchange NMR to characterise asphaltene adsorption and wettability dynamics in siliceous systems. Fuel 2018;220:692–705.
[26] Woods J, Kung J, Kingston D, Koltyar L, Sparks B, McCracken T. Canadian crudes: a comparative study of SARA fractions from a modified HPLC separation technique. Oil Gas Sci Technol Rev IFP 2008;63:59–72.
[27] Molina V D, Uribe U, Murgich J. Correlations between SARA fractions and physicochemical properties with ^{1}H NMR spectra of vacuum residues from Colombian crude oils. Fuel 2010;89:185–92.
[28] Silva S, Silva A, Ribeiro J, Martins F, Da Silva F. Chromatographic and spectroscopic analysis of heavy crude oil mixtures with emphasis in nuclear magnetic resonance spectroscopy: a review. Anal Chim Acta 2011;707:18–37.
[29] Jameel AGA, Elbaz AM, Emwas A-H, Roberts WL, Sarathy SM. Calculation of average molecular parameters, functional groups, and a surrogate molecule for heavy fuel oils using ^{1}H and ^{13}C nuclear magnetic resonance spectroscopy. Energy Fuels 2016;30:3894–905.
[30] Fan B, Khitrin A, Ermolaev K. An improved broadband decoupling sequence for liquid crystals and solids. J Magn Reson 2000;142:97–101.
[31] Mao J, Schmidt-Rohr K. Accurate quantification of aromaticity and nonprotonated aromatic carbon fraction in natural organic matter by ^{13}C solid-state nuclear magnetic resonance. Environ Sci Technol 2004;38:2680–4.
[32] Siskin M, Kelemen S, Eppig C, Brown L, Afeworki M. Asphaltene molecular structure and chemical influences on the morphology of coke produced in delayed coking. Energy Fuels 2006;20:1227–34.
[33] Boyer R, Johnson R, Krishnamurthy K. Compensation of refocusing inefficiency with synchronized inversion sweep (CRISIS) in multiplicity-edited HSQC. J Magn Reson 2003;165:253–9.
[34] Blanchard G, Maunaye M, Martin G. Removal of heavy metals from waters by means of natural zeolite. Water Res 1984;18:1501–7.
[35] Weber W, Morris J. Kinetics of adsorption of carbon from solution. J Sanit Eng Div ASCE 1963.